Journal of Inflammation Research

Dovepress
Taylor & Francis Group

Open Access Full Text Article

ORIGINAL RESEARCH

Neural-Inflammation Mechanism of Spinal Palmitic Acid Promoting Atopic Dermatitis in Mice

Jing Yang[1], Xiaoling Xue[2], Zhi Yang[1], Fei Hao[1], Bangtao Chen[3]

[1]Department of Dermatology, Third Affiliated Hospital of Chongqing Medical University, Chongqing, 401120, People's Republic of China; [2]Department of Pathogenic Biology, College of Basic Medical Sciences, Jinzhou Medical University, Jinzhou, 121001, People's Republic of China; [3]Department of Dermatology, Chongqing University Three Gorges Hospital, School of Medicine, Chongqing University, Chongqing, 404000, People's Republic of China

Correspondence: Fei Hao; Bangtao Chen, Email 651588@hospital.cqmu.edu.cn; medisci@163.com

Objective: To profile spinal medium- and long- chain fatty acids (ML-CFAs) and itch-related gene expressions (IRGEs) in dorsal root ganglion (DRG), and investigate the role of spinal palmitic acid (PA) in atopic dermatitis (AD), and its relationship with DRG and spinal extracellular signal-regulated kinase (ERK).

Methods: MC903 was applied topically to the nape of C57BL/6 mice to induce AD. Two doses of PA were administered intrathecally during MC903 treatment, and several antagonists were administered intrathecally one day before PA challenge. Transcriptome sequencing was performed on DRGs, and 36 ML-CFAs in the spinal cord were analyzed.

Results: A global upregulation of IRGEs in DRGs and increases in major ML-CFAs including PA in the spinal cord were observed in adult AD model. MC903 resulted in less severe dermatitis with weaker IRGEs in DRGs and lower spinal ML-CFAs in senile than adult mice. In adult mice, intrathecal PA injection caused acute scratches, aggravated AD, and induced stronger IRGEs in DRGs. Intrathecal injection of transient receptor potential vanilloid-1 channel (TRPV1) antagonist capsazepine or Mas-related G protein-coupled receptor D (MRGPRD) antagonist d-Pro7-ANG-(1-7) remarkably halted PA/MC903-induced dermatitis and PA-induced scratching. Administration of histamine h4 receptor antagonist JNJ7777120 only moderately alleviated dermatitis, with no notable effect on scratches. Intrathecal pan-palmitoylation inhibitor 2-Bromopalmitate moderately alleviated MC903/PA-induced lesions and spinal ERK phosphorylation. Intrathecal lidocaine markedly suppressed both lesions and ERK phosphorylation, along with a global reduction in IRGEs in DRGs. Finally, PA-induced scratches were significantly improved by intrathecal lidocaine but not 2-Bromopalmitate.

Conclusion: MC903-induced AD develops more readily in adult than senile mice, with consistent changes in IRGEs in DRG and spinal ML-CFA levels, including PA. Spinal PA promotes AD involving spinal TRPV1 and MRGPRD signaling, and IRGEs increments in DRG. Intrathecal lidocaine suppresses AD aggravated by PA via inhibiting spinal ERK phosphorylation and reducing IRGEs in DRG.

Keywords: Atopic dermatitis, Palmitic acid, Dorsal root ganglion, Spinal cord, Extracellular signal-regulated kinase, Transcriptome sequencing

Introduction

Atopic dermatitis (AD)—a chronic inflammatory dermatosis with occasional acute relapses—is characterized by intense itching and eczematous lesions on flexion (pediatric patients) or extension (geriatric patients). AD disease burden is the highest among all dermatoses, affecting individuals of nearly all age groups, with a rising incidence worldwide. Notably, the global prevalence of AD was 2.23% in 2019 and has remained relatively stable since 1990.[1] The latest data have highlighted 3.96% and 1.95% global prevalence of AD in children and adults, respectively.[2] Based on the Bayesian age-period-cohort model, the predicted age-standardized prevalence rate of AD in China may reach 13943.6/million in males and 16036.9/million in females by 2030.[3] Although global epidemiological data on AD in older individuals is limited, its diagnosis is increasingly observed in clinical practice.[4]

Received: 1 March 2025
Accepted: 10 June 2025
Published: 17 June 2025

AD is well recognized as a Th2-inflammation-driven disease with systemic components. Recalcitrant pruritus leads to substantial sleep disturbances and psychosocial dysfunction. High heterogeneity of AD contributes to the difficulty in its precise clinical management,[5] with lesion patterns in older individuals being significantly different from those in children.[6] Our previous review summarized the characteristics of skin aging in AD, emphasizing the need to consider age in relation to AD pathogenesis and treatment.[7] Major advances in understanding of the pathophysiology of AD support the concept that its onset or progression involves multiple factors, including genetic predisposition, impaired skin barrier, abnormal immunity, skin microbial dysbiosis, and psychological problems. These factors synergistically cause skin neuroinflammation, where differential activation of diverse membrane receptors and ion channels on mast cells, keratinocytes, and sensory nerve endings shapes AD heterogeneity.[8] Specifically, the discovery of Mas-related G protein-coupled receptor (MRGPR) and transient receptor potential (TRP) superfamily has further enriched the diversity of neuroinflammation.[9,10]

Dorsal root ganglion (DRG) and spinal cord are closely connected anatomically, and short hairpin RNA (shRNA) can be successfully delivered to both sites via intrathecal administration at the L5–L6 lumbar region.[11] These structures are responsible for itch signal processing and are therefore involved in the pathogenesis of pruritic dermatosis, making them potential targets for biological therapeutics. Interleukin (IL)-31RA and cysteinyl leukotriene receptor 2 (CysLTR2) on DRG mediate chronic itch in AD.[12,13] However, transcriptomics or proteomics of DRG are recommended to comprehensively understand the role of DRG in AD or itch models induced by specific topical agents. Recent studies also reported the involvement of spinal extracellular signal-regulated kinase (ERK) in histamine-dependent or -independent itching.[14,15] Therefore, intrathecal administration of drugs directly acting on the spinal cord or DRG may be an alternative avenue for the treatment of extremely refractory AD or itching, although the safety of long-term application remains underexplored.

Palmitic acid (PA)—a 16-carbon long-chain (C16:0) saturated fatty acid—is present in common dietary fats and is also synthesized endogenously.[16] PA-mediated protein palmitoylation, in which PA is covalently attached to the cysteine residues in proteins through a thioester bond, plays crucial roles in biological homeostasis.[17] Recent studies have confirmed the role of protein palmitoylation in maintaining skin barrier integrity and in microbial encounter-induced dermatitis.[18,19] The biological effect of PA is associated with ERK phosphorylation in non-neuronal cells.[20] Specifically, PA is present in various organs, and its origin and metabolic fate in the brain have been summarized previously.[21] Furthermore, PA may be present in the spinal cord and may be influenced by pathological conditions.[22] However, the levels of spinal PA and its effect on the spinal cord or DRG in pruritic dermatosis development are still largely unclear. This study aimed to profile the spinal medium- and long-chain fatty acids (ML-CFAs), including PA, and the expressions of itch-related genes in the DRG in adult and senile murine AD models. We also investigated the role of spinal PA in AD phenotypes and scratching behavior, as well as their relationship with DRG and spinal ERK in adult mice, to refine strategies for more precise AD management.

Methods

Materials

The animal experiments and procedures in this study were approved by the Ethics Committee of Chongqing University Three Gorges Hospital. Furthermore, the experiments adhered to the guidelines on animal protection, Laboratory animal - Guideline for ethical review of animal welfare (GB/T 35892–2018, China). The wild-type (WT) adult (aged 8–10 weeks) and senile (aged 70–72 weeks) C57BL/6 mice were purchased from Beijing Vital River Laboratory Animal Technology Co., Ltd. All mice were bred and housed in ventilated cages in the same housing unit at 25 ± 2 °C, 50 ± 5% humidity, and light/dark cycle of 12 h.

MC903(#HY-10001), Chlorpheniramine(#HY-B0286), GSK189254(#HY-14111), HC-030031(#HY-15064) and capsazepine (#HY-15640) were purchased from MCE (USA). JNJ7777120 (#J3770) and 2BP (#21604) were purchased from Sigma-Aldrich (St Louis, MO, USA). Lidocaine(#S1357) was provided by Selleck (Houston, TX, USA). d-Pro7-ANG -(1-7) was synthesized in Hongtide (Shanghai, China). Mouse IL-13 (#MM-0173M2, MEIMIAN, Jiangsu, China), mouse thymic stromal lymphopoietin (TSLP; #MM-45118M2, MEIMIAN, Jiangsu, China), and mouse total IgE (#ab157718,

Abcam) kits were used for enzyme-linked immunosorbent assay (ELISA). Antibodies included anti-phospho-ERK (#AP0472, Abclonal) and anti-GAPDH (#A19056, Abclonal). The other materials used were DMSO (#D806645, Macklin, Seattle, WA, USA), RIPA lysis solution (#P0013B, Beyotime, Beijing, China), bicinchoninic acid kit (#P0009, Beyotime), PVDF membrane (Millipore, #IPVH09120, MA, USA), enhanced chemiluminescence detection kit (#WBKLS, Millipore), 4% paraformaldehyde (#P885233, Macklin), paraffin (#P815701, Macklin), hematoxylin and eosin (HE) kit (#DH0020, Leagene, Beijing, China) and toluidine blue (TB) dye (#D-034-1-1, JIANCHENG, Nanjing, China).

AD Mouse Model and Interventions

Adult or senile offspring were used for the experiments. On day 0, hairs were removed from the neck and upper back, exposing an area of approximately 2×2 cm^2. MC903 powder was dissolved in 100% ethanol to a concentration of 45 mm and further diluted to 45 μM with saline as required.[15,23] From day 1, 20 μL/cm^2 MC903 (45 μM) was topically applied to the exposed skin areas of mice for 10–14 consecutive days, as required. Furthermore, 3% pentobarbital sodium (5 μL/g) was intraperitoneally injected to induce anesthesia, and related samples, including serum, skin lesions, spinal cord, and DRGs, were collected. During MC903 application, PA (5 μg in 10 μL saline) was intrathecally administered at the lumbar level (L4 and L5) on days 3 and 7 using a 30-gauge needle. Additionally, on days 2 and 5, intrathecal injection of chlorpheniramine (2 μg in 10 μL saline), GSK189254 (5 μg in 10 μL saline), JNJ7777120 (2 μg in 10 μL saline), HC-030031(5 μg in 10 μL saline), capsazepine (5 μg in 10 μL saline), d-Pro7-ANG-(1-7) (5 μg in 10 μL saline), 2BP(5 μg in 10 μL saline), or lidocaine (1%, 10 μL) was also administered in different settings, as indicated in the figure legend. These inhibitors were also administered intrathecally in experiments assessing PA-induced acute scratching without topical MC903 application. The inhibitors were administered 24 h before PA injection, and the scratching behaviors were recorded for 10 min following PA injection. Since mice in the cage often run back and forth, a single video recording was insufficient to capture all the scratching behaviors. Therefore, behaviors in this study were recorded manually on site.

Western Blotting

Fresh cervical and upper thoracic spinal cord were immediately frozen and stored in liquid nitrogen until use. The frozen spinal cord was weighed and lysed using strong RIPA lysis solution containing protease and phosphatase inhibitors in pre-cooled tissue lyser for 20 min. Next, the total proteins in the lysates were extracted via centrifugation at 12,000 × g for 15 min at 4 °C. A bicinchoninic acid kit was used to determine protein concentration, and 40 μg of protein were subjected to 10% SDS–PAGE and transferred onto a 0.45-μm PVDF membrane. After blocking with bovine serum albumin, the membranes were incubated overnight at 4 °C with primary antibodies (1:1000), including phosphorylated ERK and GAPDH antibodies. The target protein was visualized using an enhanced chemiluminescence detection kit. Each immunoblot assay was performed three times, and one representative blot is shown.

RNA-Sequencing Analysis

Bilateral C2 to T2 DRGs from mock- or MC903-treated WT mice were immediately collected after skin tissue collection, and the attached nerve fibers were removed under a microscope. Total RNA from fresh DRGs was extracted using TRIzol reagent (Invitrogen) following the manufacturer's instructions, and DNase I was used to eliminate DNA contamination. The quality and integrity of the isolated RNAs were assessed using a NanoDrop ND-1000 Spectrophotometer (Nucliber). The Ion Total RNA-Seq Kit V2 (Life Technologies, USA) was used to construct a sequencing library for each RNA sample following the manufacturer's instructions. The cDNA libraries were sequenced using an Illumina HiSeq2000 (Majorbio Biotechnology Company, China). Pipeline for RNA sequencing data analysis and identification of differentially expressed genes (DEGs) were conducted as previously reported by Sengupta et al and Liu et al.[24,25] Raw data were deposited in the National Center for Biotechnology Information Sequence Read Archive (accession number: PRJNA1263495).

Gas Chromatography Mass Spectrometry (GC-MS)

GC-MS was used to simultaneously determine 36 ML-CFAs. Briefly, 100 mg spinal cord was ground with 1 mL of dichloromethane/methanol (v/v = 1/1), ultrasonicated, and centrifuged at low temperature. Thereafter, 0.5 mL sodium hydroxide methanol solution (0.5 mol/L) and 0.5 mL n-hexane were sequentially added to the supernatant, and the solution was incubated. Finally, the hexane layer was collected for GC–MS analysis (Majorbio, Shanghai, China). GC–MS settings included an Agilent DB-FastFAME capillary column, 20 m × 0.18 mm × 0.20 μm; carrier gas, 99.999% helium, 1 mL/min; sample injection volume, 1 μL; splitting mode, 50:1; and GC column temperature programming, 80 °C for 30s, increasing to 175 °C within 1.35 min, increasing to 230 °C within 8 min, and 230 °C for 2 min.

Histological Stain

Fresh skin lesions were cut into 0.5×0.5 cm^2 sections, fixed in 4% paraformaldehyde for 24 h, and embedded in paraffin. Deparaffinized and rehydrated slices were stained with HE for observing the morphology and inflammatory infiltration. Additionally, TB staining was used to observe mast cell degranulation in tissues.

Elisa

Serum IgE, skin IL13 and TLSP levels were determined by ELISA using commercial kits following the manufacturer's instructions.

Statistical Analyses

Bioinformatic analyses of the transcriptome data and GC–MS data were performed using a free online platform of Majorbio cloud platform (cloud.majorbio.com).[26] GraphPad Prism 5.0® software package (San Diego, California) was used for statistical analysis. One-way ANOVA followed by Bonferroni's or Dunnett's multiple comparisons post hoc tests were used to analyze differences in different groups. Student's *t*-test was used for determining differences between the groups. Two-sided $P < 0.05$ was considered statistically significant.

Results

Transcriptomics of DRGs in Adult and Senile Mice with AD

Following the topical application of the same dosage and for the same duration of MC903 to the nape of adult and senile mice, the macroscopic skin lesions at day 14, epidermal thickening and inflammatory cell infiltration observed using HE staining, and mast cells degranulation observed by TB staining were more notable in adult mice than in senile mice (Figure 1A). We also collected bilateral murine C1 to T2 DRGs for transcriptomics analysis to identify the neuronal genes associated with AD-like dermatitis among adult and senile mice. Compared with the mock treatment, 56980 DEGs (including 63 upregulated and 155 downregulated) were identified in MC903-treated adult mice (Supplmentary Figure 1A). Furthermore, compared with the adult mice, 56980 DEGs (including 236 upregulated and 97 downregulated) were identified in MC903-treated senile mice (Supplmentary Figure 1B). We then compared significantly altered genes related to itch or pain signaling neurotransmission-related receptors, ion channels, neuropeptides, neurotrophins, and interleukins. All downregulated genes reduced by <50%, whereas most upregulated genes increased by <1-fold, except *Mrgpra3, Mrgprb4*, and *Mrgprb5*, which were upregulated 1- to 2-fold in the AD model compared to adult controls (Figure 1B; Supplmentary Table 1). In AD models, compared with the adults, senile mice exhibited a narrower range of receptor gene expression, including >50% reductions in *Mrgpra3, Mrgprb4*, and *Mrgprb5*, 34% in *Calcb*, and 54.0% in *Nts*. Conversely, *Bdnf, Kcnmb2*, and *Kcnmb4os2* were upregulated by 1- to 2-fold (Figure 1C; Supplmentary Table 2). These findings reveal possible neuroinflammation mechanisms underlying AD and its heterogeneity by age.

Spinal ML-CFAs in Adult and Senile Mice with AD

In total, 36 ML-CFAs in spinal cord were identified using GC–MS. Samples from different groups were clearly separated but clustered within groups (Figure 2A). The expression of most ML-CFAs was relatively consistent within the group except for C18:3n3 (alpha-linolenate), C13:0 (tridecanoate), C8:0 (caprylate), C12:0 (laurate), C10:0 (caprate), C20:2 (11,14-

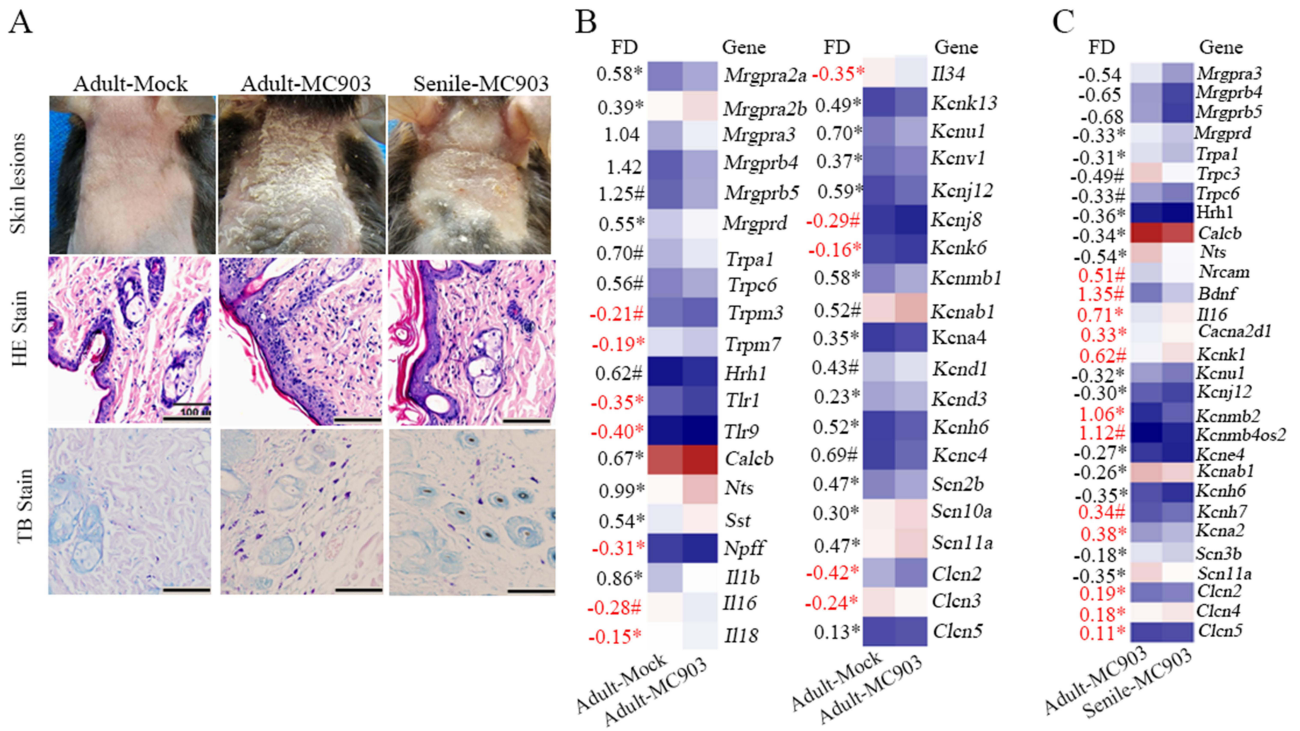

Figure 1 Difference in MC903-treated adult and senile mice. MC903 (45 μM; 20 μL/cm^2) was topically applied to the exposed skin areas of 8–10-week-old mice (n = 6 per group) for 14 consecutive days, and skin lesions were photographed. Mice were then anesthetized via intraperitoneal pentobarbital sodium, and the skin lesions and DRGs were obtained. (**A**) Skin lesions and HE and TB staining results (scale bar = 100 μm). DRGs (n = 4 per group) were used for transcriptome sequencing. (**B**) DEGs identified between mock and MC903-treated adult mice are shown. The numbers are equal to the difference (obtained by subtracting the data in column one from that in column two) divided by that in column one; the minus sign represents a decrease and the corresponding numbers of the down-regulated genes are marked in red. (**C**) The DEGs between adult and senile mice in the context of MC903 treatment are shown. Numbers are represented the same as those in Figure 1B; the minus sign represents a decrease and the corresponding numbers of the up-regulated genes are marked in red. Student's *t*-test was used for statistical analysis, * $P < 0.05$, #$P < 0.01$, not labelled $P < 0.001$.

eicosadienoate), C20:3n6 (homogamma linolenate), and C22:2 (docosadienoate) (Figure 2B). Other ML-CFAs at levels >1 μg/mg were C18:1n9t (elaidate, Figure 2C), C18:0 (stearate, Figure 2D), C16:0 (palmitate, Figure 2E), and C20:1t (trans-11-Eicosenoate, Figure 2F). The abundances of these ML-CFAs in MC903-treated adult mice were significantly higher than in both mock-treated adult mice and MC903-treated senile mice.

Intrathecal Injection of PA Caused Acute Scratches and Aggravated AD-Like Dermatitis

To determine the effect of spinal PA on AD-like lesions and pruritus, intrathecal injection of PA was applied during MC903 treatment in adult mice. At day 10, more skin scales, severely hypertrophied epidermis, and more inflammatory cell infiltration and mast cell degranulation in dermis were observed in PA-treated AD models compared to the corresponding solvent-treated group (Figure 3A). ELISA results showed similar levels of total serum IgE between MC903 and MC903 + PA groups (275.04 ± 87.61 vs 301.15 ± 97.64 ng/mL, P = 0.636). However, remarkably higher levels of skin IL-13 ($P < 0.01$, Figure 3B) and TSLP ($P < 0.05$, Figure 3C) were observed in the MC903 + PA group. In addition, compared to the control, the number of scratches within 10 min significantly increased in intrathecal PA-administered mice without topical MC903 (6.17 ± 1.16 vs 29.33 ± 6.25, $P < 0.001$). Transcriptome analysis revealed 2092 upregulated and 3868 downregulated DEGs in DRGs from adult AD models following intrathecal PA administration (Supplmentary Figure 1C). Specifically, 14 genes were elevated 5- to 10-fold (including *Asic1, Asic2*, and *Asic3*) and 45 were elevated 2- to 5-fold (including *Mrgpra3, Mrgprd, Mrgpre, Nptx2, Trpv1, Trpv2, Piezo2*, and *Gal*). Meanwhile, some DEGs, including toll-like receptor (*Tlr*)*1, Tlr2, Tlr4, Tlr6, Tlr7, Tlr8, Tlr9*, and *Tlr13*, showed >50% reductions (Figure 3D; Supplmentary Table 3).

https://doi.org/10.2147/JIR.S525663

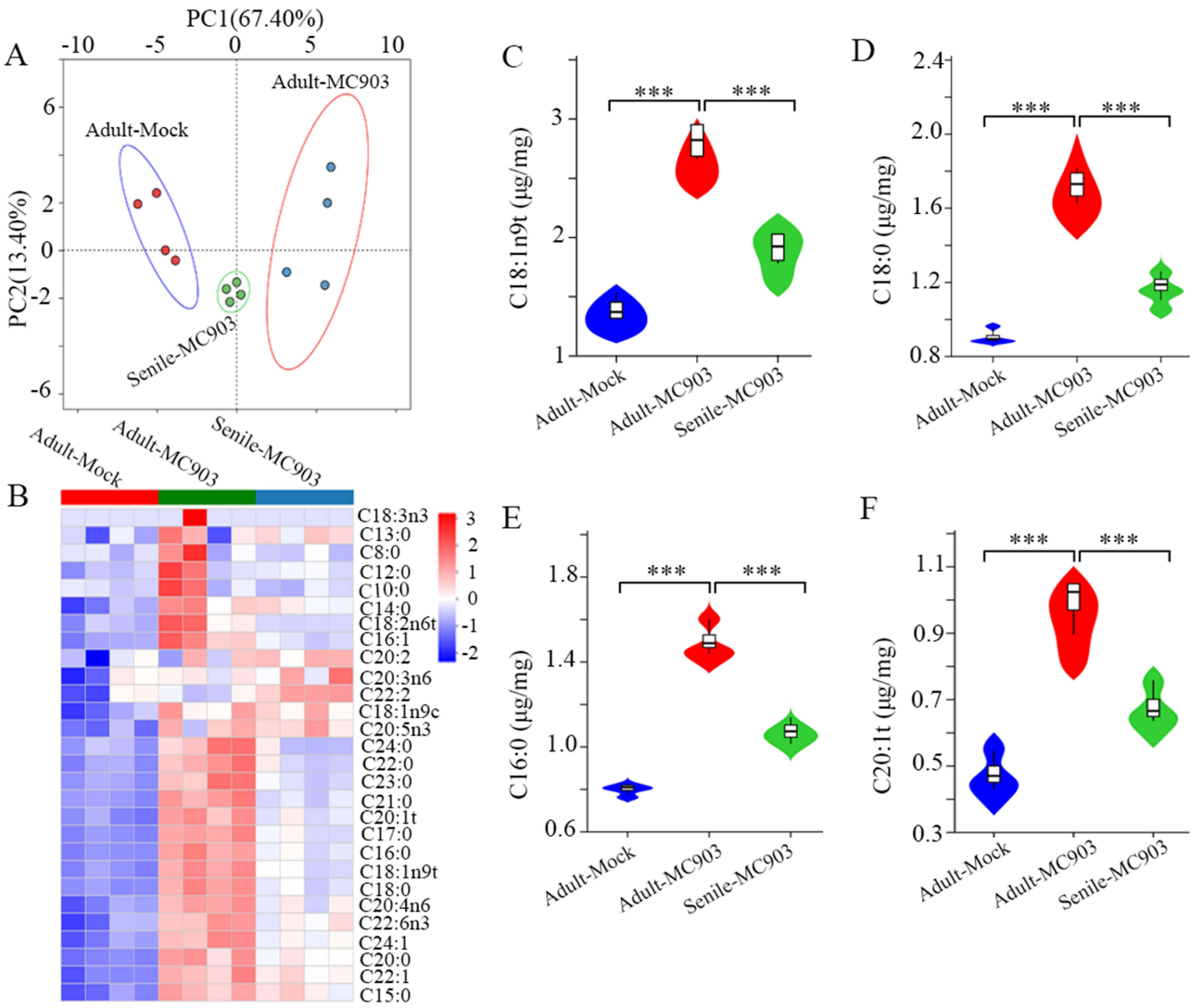

Figure 2 Comparisons of spinal ML-CFAs levels in the three groups. Fresh spinal cords from the mice (n = 4 per group) in Figure 1 were collected to identify 36 ML-CFAs using GC–MS. (**A**) Principal component analysis. (**B**) Heatmap analysis of each fatty acid in each sample of the three groups. Comparisons of the average levels of the four fatty acids with the highest abundance in the three groups were performed, and C18:1n9t (**C**), C18:0 (**D**), C16:0 (**E**), and C20:1t (**F**) are shown. One-way ANOVA with Bonferroni's test was used for statistical analysis, *** $P < 0.001$.

Spinal TRPV1 and MRGPRD Signaling Contributed to the Function of Intrathecal PA

To further clarify the possible neuroreceptors involved in MC903-induced AD-like skin lesions following exogenous PA treatment, histamine h1 receptor (H1R) antagonist chlorpheniramine, H3R antagonist GSK189254, H4R antagonist JNJ7777120, TRP ankyrin 1 antagonist HC-030031, TRPV1 antagonist capsazepine, or MRGPRD antagonist d-Pro7-ANG-(1-7) were intrathecally applied. Compared to the control solvent, AD phenotypes, including macroscopic scales, epidermal thickness, inflammatory cell infiltration, and mast cell degranulation in the dermis were significantly alleviated in capsazepine- and d-Pro7-ANG-(1-7) administered groups at day 10 and moderately alleviated in the JNJ7777120 group (Figure 4). Moreover, intrathecal PA-induced scratches within 10 min in mice without MC903 application were similar to those treated with solvent (31.17 ± 5.42), chlorpheniramine (29.67 ± 6.06), GSK189254 (27.83 ± 2.93), JNJ7777120 (30.83 ± 4.96), and HC-030031 (30.67 ± 6.15), but remarkably reduced in capsazepine (15.67 ± 2.58) and d-Pro7-ANG-(1-7) (14.33 ± 2.25) groups. These data suggest that spinal TRPV1 and MRGPRD signaling contribute to the effects of intrathecal PA.

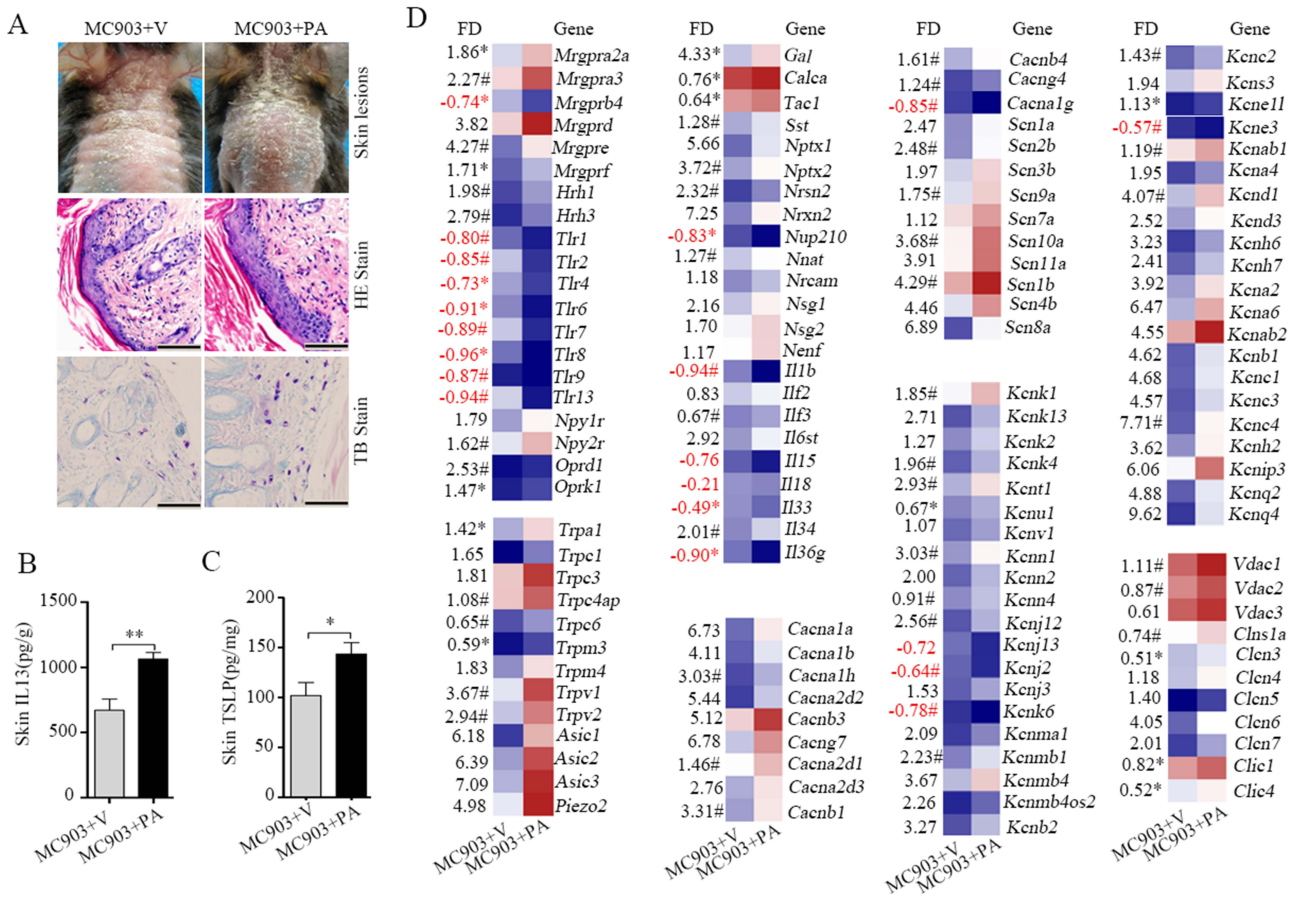

Figure 3 Effect of intrathecal PA injection on AD-like dermatitis and spontaneous scratches. MC903 (45 μM; 20 μL/cm^2) was topically applied to the exposed skin areas of 8–10-weeks-old mice (n = 6 per group) for 10 consecutive days, and PA (5 μg in 10 μL) or corresponding solvent (SVT) in equal volume was intrathecally injected on days 3 and 7. (**A**) Skin lesions and histological staining results at day 10 (scale bar = 100 μm). (**B**) Skin IL-13 levels at day 10. (**C**) Skin TSLP levels at day 10. DRGs (n = 4 per group) were used for transcriptome sequencing. (**D**) The DEGs between the two groups are shown, and the numbers are represented same as those in Figure 1B; the minus sign represents a decrease and the corresponding numbers of the down-regulated genes are marked in red. Student's *t*-test was used for statistical analysis, * $P < 0.05$, ** or # $P < 0.01$, not labelled $P < 0.001$.

Intrathecal 2BP or Lidocaine Inhibited Dermatitis via ERK Inhibition

Owing to the pro-palmitoylation property of PA, the pan-palmitoylation inhibitor (2BP) was further intrathecally administered to mice with or without MC903 application. 2BP significantly decreased MC903/PA-induced AD-like lesions, skin histopathological changes, and spinal ERK phosphorylation (Figure 5A and B), but did not alter the PA-induced acute scratches within 10 min (Figure 5C). Additionally, intrathecal application of lidocaine, the drug widely used in the clinic, could markedly suppress AD-like lesions (Figure 5A), spinal ERK phosphorylation (Figure 5B), and acute scratches (Figure 5C). Overall, intrathecal lidocaine supplementation upregulated 4360 and downregulated 2708 DEGs in DRGs from MC903/PA-treated models (Supplmentary Figure 1D). Lidocaine decreased almost all selected genes by >50%, but significantly upregulated *Tlr1, Tlr6, Tlr8, Tlr9*, and *Cacna1g* expressions (>5-fold) (Figure 6; Supplmnetary Table 4).

Discussion

Skin neuroinflammation or neuro-immune circuit, in which skin resident cells and cutaneous sensory nerve endings innervating the skin communicate through inflammatory mediators or neurotransmitters, is well established as the most critical pathophysiology for recalcitrant chronic itching and treatment resistance in AD.[27,28] DRG, the only relay station for central and peripheral itch signals, is the key target for exploring neural mechanisms in different animal models of AD.[29] However, transcriptome data of DRGs from AD-like animals remains unavailable. The present study addresses

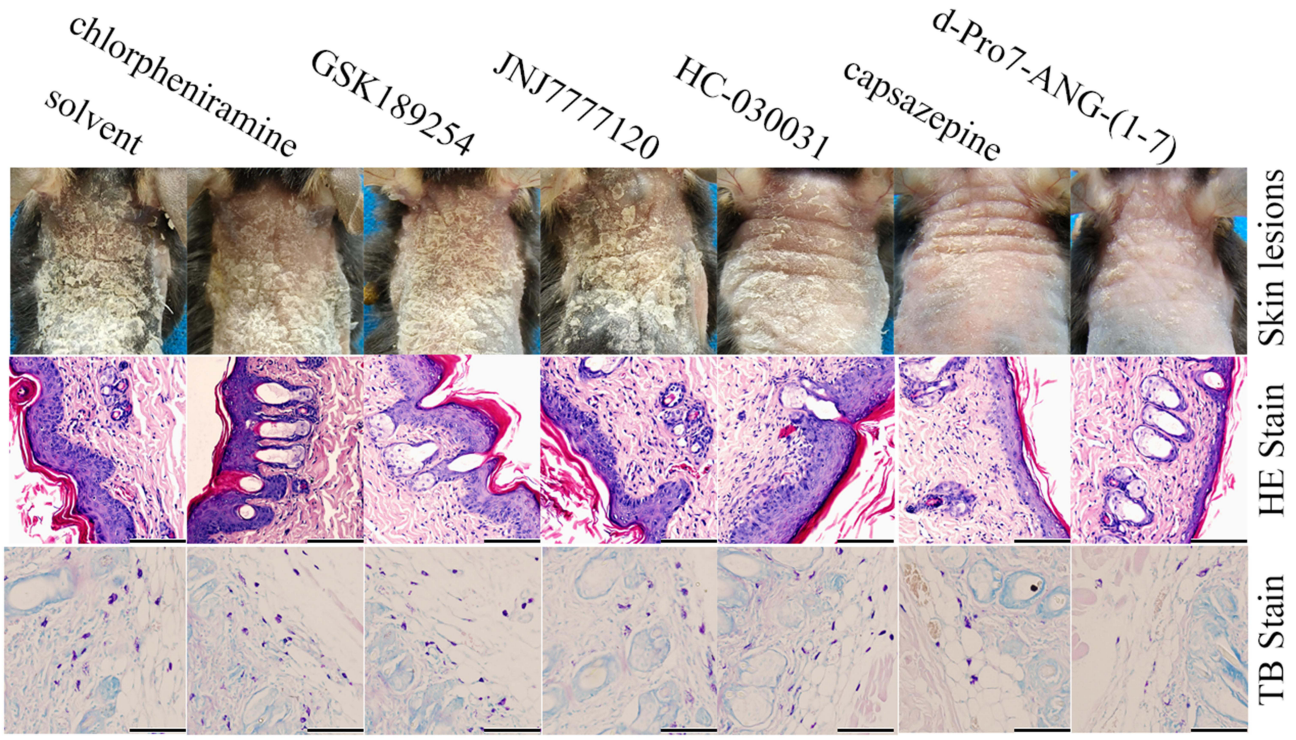

Figure 4 Effect of several itch receptor antagonists on PA/MC903-induced dermatitis. MC903 (45 μM; 20 μL/cm^2) was topically applied to the exposed skin areas of 8–10 weeks-old mice (n = 6 per group) for 10 consecutive days. On days 2 and 6, intrathecal injection of solvent, chlorpheniramine (2 μg in 10 μL saline), GSK189254 (5 μg in 10 μL saline), JNJ7777120 (2 μg in 10 μL saline), HC-030031(5 μg in 10 μL saline), capsazepine (5 μg in 10 μL saline), or d-Pro7-ANG-(1-7) (5 μg in 10 μL saline) was administered. On days 3 and 7, all the mice received intrathecal PA injections. Skin lesions and histological staining results are presented (scale bar = 100 μm).

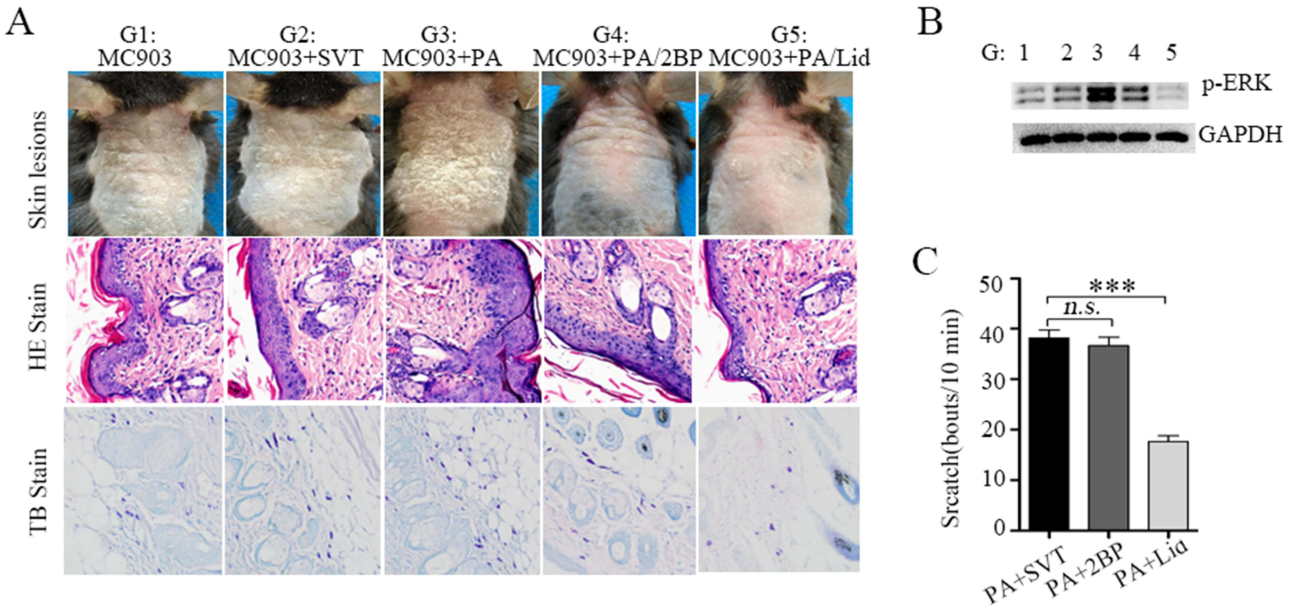

Figure 5 Effect of intrathecal 2BP or lidocaine on dermatitis, scratches, and spinal ERK phosphorylation. MC903 (45 μM; 20 μL/cm^2) was topically applied to the exposed skin areas of 8–10 weeks-old mice (n = 6 per group) for 10 consecutive days. On days 2 and 6, intrathecal injection of SVT, 2BP (5 μg in 10 μL saline), or lidocaine (Lid, 1%, 10 μL) was administered. On days 3 and 7, intrathecal injection SVT or PA was administered. (**A**) Skin lesions and histological staining results at day 10 (scale bar = 100 μm). (**B**) Spinal phosphorylated-ERK levels at day 10. (**C**) 2BP (5 μg in 10 μL saline) or lidocaine (1%, 10 μL) was intrathecally pre-administered to 8–10-week-old mice (n = 6 per group). Intrathecal PA (5 μg in 10 μL) or corresponding SVT in equal volume was administered 24 h later. The scratching behaviors within 10 min after PA injection were monitored. One-way ANOVA followed by Dunnett's test was used for statistical analysis, ***$P < 0.001$, n.s. $P > 0.05$.

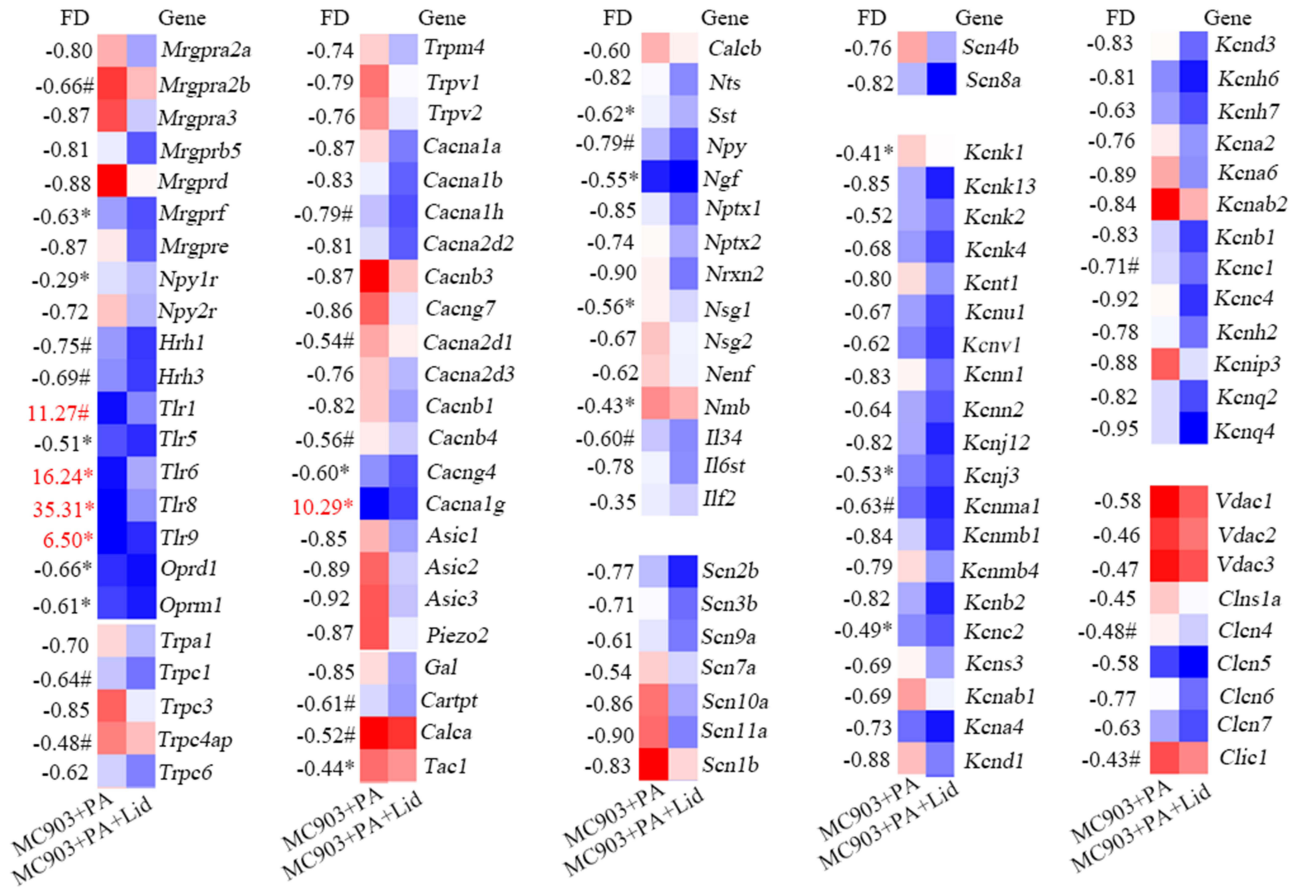

Figure 6 DEGs between the two groups. DRGs from MC903 + PA (n=2) and MC903 + PA/lidocaine (n = 4) groups were used for transcriptome sequencing. The DEGs between the two groups are shown, and the numbers are represented the same as those in Figure 1B; the minus sign represents a decrease and the corresponding numbers of the up-regulated genes are marked in red. Student's *t*-test was used for statistical analysis, **P* < 0.05, #*P* < 0.01, not labelled *P* < 0.001.

this gap by demonstrating that the mRNA levels of itch-related receptors (*Mrgpra, Mrgprb, Mrgprd, Trpa1, Trpc6* and *Hrh1*), inflammatory mediators (*Calcb, Nts, Sst* and *IL1β*), and several subtypes of ion channels (sodium, potassium, chloride) were significantly elevated in DRGs of an AD-like adult murine model. However, further analysis is required to determine the positive role of Mrgpra in itching or dermatitis. Although one or more of these altered, and even unaltered, genes may individually contribute to pruritic dermatoses, they may also act synergistically. The potential complex cross-talk among them warrants careful consideration when interpreting or citing these findings. More recently, the neural circuits in the spinal cord and brain in pruritic dermatosis have been gradually unveiled.[30–33] However, little is known about the microenvironmental factors affecting neural circuits apart from neurotransmitters and inflammatory mediators. In this study, we profiled 36 spinal ML-CFAs. Notably, many ML-CFAs were elevated in adult AD-like mice in our study, which has not been reported previously.

Preventing AD in the older individuals poses a significant challenge, given its rising prevalence and diverse phenotypes.[34] Inflammaging, characterized by a persistent low level of pro-inflammatory biomarkers (including C-reactive protein, IL1β, IL6, and tumor necrosis factor α) in serum or skin is a typical characteristic of immunosenescence in aged populations. Current evidence shows that with advancing age, AD lesions exhibit increased Th1/Th17 cytokines and terminal keratinocyte differentiation markers (filaggrin and loricrin), as well as decreased epidermal hyperplasia markers (Ki16 and Ki67) and Th2/Th22 cytokines.[7] In this study, we observed weakened AD phenotypes in aged mice following topical MC903 application. To our knowledge, this is the first study to elucidate the neuromechanisms underlying age-related heterogeneity in AD models using DRG transcriptomics. Almost all the genes related to itch signal processing were significantly downregulated in aged mice compared to adults, except for *Bdnf, Kcnmb2*, and *Kcnmb4os2*. Furthermore, *Calcb* and *Nts* also reduced with aging, consistent with the previous research.[35] Additionally,

spinal ML-CFA levels, including those of C18:1n9t (Elaidate), C18:0 (Stearate), C16:0 (Palmitate), and C20:1 (Trans-11-Eicosenoate), in aged AD mice were also lower than those in the adult AD mice. These alterations likely contribute to the age-related heterogeneity in clinical AD phenotypes and offer important insights for clinical management, particularly in selecting and evaluating biological therapeutics.[36]

Spinal cord injury caused upregulation of spinal PA in rabbit.[22] Conversely, Ewan et al demonstrated that fatty acid biosynthesis, including the generation of palmitic acid (PA), is downregulated following spinal cord injury in purified spinal sensory neurons from mice, thereby limiting axon regenerative capacity. This suggests that maintaining spinal PA homeostasis may facilitate neuronal regeneration, a concept supported in part by the neuroprotective effects of palmitoylethanolamide, an amide derivative of ethanolamine and PA.[37,38] However, studies exploring the biological functions of the spine PA outside the context of spinal cord injury are lacking. In our study, intrathecal PA injection induced acute scratches, exacerbated MC903-induced AD-like lesions, and promoted skin Th2 inflammation independent of total IgE. Unlike spinal PA, a PA-rich diet-induced obesity also exacerbates murine AD-like dermatitis, and PA can increase TSLP expression in keratinocytes.[39,40] Moreover, oropharyngeal inoculation with PA in a mouse model, intranasally treated with IL-13, also aggravates airway Th2 inflammation.[41] TLR2/4 signaling is essential for PA-induced inflammation in non-neuronal cells.[42] However, almost all *Tlr* subtypes genes, including *Tlr2* and *Tlr4*, were remarkably downregulated in DRG from AD-like mice following intrathecal PA administration, suggesting that PA-induced spinal neuroinflammation is independent of TLRs. Neuro-mechanistically, intrathecal PA administration could upregulate almost all the potential itch-related genes in DRGs, including receptors (*Mrgpr, H1/3r* and *Trpv1*), ion channels (*Asic*, calcium, sodium, potassium, and chloride), and neuropeptides. Further evidence confirmed the crucial role of MRGPRD and TRPV1 signaling in DRG and/or spinal cord in both PA/MC903-induced AD-like dermatitis and PA-induced acute itch.

To our knowledge, the role of $TRPV1^+$ nerves in the development of inflammatory skin disease and related itch has been extensively demonstrated. $MRGPRD^+$ nerves, which innervate the outermost viable epidermal layer and terminate in the nonpeptidergic lamina of the spinal cord dorsal horn,[43] have also been implicated in transmitting both nonhistaminergic itching in allergic contact dermatitis and mechanical pain signals.[44–46] Interestingly, in situ hybridization studies have demonstrated MRGPRD co-expression in a subpopulation of $TRPV1^+$ human DRG neurons,[47] explaining why both the MRGPRD and TRPV1 signaling in DRG and/or the spinal cord contribute to PA-induced acute itch and dermatitis exacerbation. However, this evidence is insufficient to confirm that MRGPRD is the direct receptor for PA. Recent findings suggest that PA may instead bind to CysLTR2,[48] which is expressed in DRG neurons and mediates leukotriene C4-driven acute itch in pruritus in models of AD or non-AD.[12,49] Therefore, MRGPRD signaling may function downstream of CysLTR2 activation.

Pruritus is the key feature in chronic dermatitis progression. In recent years, several research teams have focused on the critical role of spinal ERK expression or phosphorylation in chronic itch signal processing under different conditions. Matsuo et al reported steady-state ERK phosphorylation in spinal neurokinin B- or urocortin3-expressing neurons and demonstrated that chronic allergic dermatitis further enhanced ERK activation. These findings highlighted that spinal ERK2 deficiency impairs both chemical itch induced by histamine and mechanical itch triggered by histamine or IL-31.[50] Additionally, persistent ERK phosphorylation in spinal GRPR-, NPRA-, NMBR-, and sst2A-expressing neurons was observed across four mouse models of chronic itch, including those induced by squaric acid dibutylester, imiquimod, MC903, and acetone–ether–water. This sustained activation was alleviated by intrathecal injection of U0126 or PD0325901.[15] In hepatocytes, PA induced ERK phosphorylation in a dose- and time-dependent manner.[20] In the present study, intrathecal PA injection significantly enhanced spinal ERK phosphorylation in MC903-induced AD-like dermatitis. Therefore, spinal ERK phosphorylation could be a promising target for the treatment of recalcitrant AD, aligning with evidence from studies using Angelica Yinzi.[51] Lidocaine, a widely used anesthetic, has been reported to alleviate skin lesions and itch in patients with AD and MC903-induced AD-like murine models by modulating subpopulations of sensory neurons innervating skin and suppressing the release of the neuropeptide calcitonin gene-related peptide.[52] In our study, intrathecal injection of lidocaine significantly inhibited PA/MC903-induced AD-like dermatitis by inhibiting spinal ERK phosphorylation—a mechanism previously observed in α-amino-3-hydroxy-5-methyl-4- izoxazolepropionic acid- or capsaicin-activated rat dorsal horn neurons.[53] Additionally, the global inhibition of potential itch-related genes in DRG

by lidocaine may also contribute to its protective effects in mice against PA/MC903-induced AD-like dermatitis. Nevertheless, the relationship between intrathecal lidocaine-mediated inhibition of PA-induced acute scratching and spinal ERK phosphorylation warrants further investigation. PA promotes protein palmitoylation under various conditions.[17,54] Intrathecal pan-palmitoylation inhibitor 2BP suppressed ERK phosphorylation and alleviated MC903/PA-induced AD-like lesions in the present study. This suggests that spinal protein palmitoylation may contribute to chronic pruritus and dermatitis. Importantly, 2BP has also been reported to inhibit ERK phosphorylation in hypopharyngeal squamous cells and neural stem/progenitor cells.[55,56] However, 2BP did not influence PA-induced acute scratching within 10 min, possibly because transient PA or 2BP exposure does not immediately affect spinal protein palmitoylation.

Nevertheless, certain questions still remain unanswered. First, palmitoylation proteomics is crucial to verify whether intrathecal PA enhances protein palmitoylation in the spinal cord or DRGs. The functional relevance of this modification in AD phenotype should be further validated. Specifically, direct palmitoylation targets such as TRPV1, Ras, and Gα subunits in AD models following intrathecal PA administration should be evaluated using acyl-biotin exchange (ABE) methods. Second, spinal ERK phosphorylation might not sufficiently represent the neuroinflammatory effects of PA. Comprehensive proteomic profiling is imperative to uncover broader signaling pathways. Third, many newly discovered altered genes in DRGs from transcriptomics analysis in multiple experimental settings, which were not examined in the current study, may provide a new perspective underlying the neural mechanisms of AD. Finally, validating the findings in mice with conditional knockout of gene *Trpv1, Mrgprd*, or *Erk* at the spinal cord or DRG level would significantly strengthen the conclusions.

Conclusions

This study demonstrates that MC903-induced AD is more susceptible to development in adult mice than in senile mice, with consistent alterations in itch-related gene expressions in DRG and spinal ML-CFAs. Spinal PA induces acute scratching and exacerbates AD, involving TRPV1 and MRGPRD signaling in DRG and/or spinal cord. Inhibition of spinal ERK phosphorylation and downregulation of itch-related genes expressions are possibly implicated in the suppression of PA-aggravated AD mediated by intrathecal lidocaine.

Data Sharing Statement

The data supporting the findings of this study are available from the corresponding author upon reasonable request.

Ethics Approval

The animal experiments and execution in this study were approved by the Ethics Committee of Chongqing University Three Gorges Hospital.

Acknowledgments

We would like to thank Delu Che (Department of Dermatology, Northwest Hospital, The Second Hospital Affiliated to Xi'an Jiaotong University) for his support of our study.

Funding

This work was supported by grants from the National Natural Science Foundation of China (82003337 and 82373479), Medical youth top-talent project in Chongqing (YXQN202462), Doctoral Program in Wanzhou District (wzstc-20220122) and Funding for Postdoctoral Fellowships in Chongqing (55012).

Disclosure

The authors report no conflicts of interest in this work.

References

1. Faye O, Flohr C, Kabashima K, et al. Atopic dermatitis: a global health perspective. *J Eur Acad Dermatol Venereol*. 2024;38(5):801–811. doi:10.1111/jdv.19723

2. Tian J, Zhang D, Yang Y, et al. Global epidemiology of atopic dermatitis: a comprehensive systematic analysis and modelling study. *Br J Dermatol*. 2023;190(1):55–61. doi:10.1093/bjd/ljad339
3. Zhou J, Chen H, Zhou S, et al. Trends in atopic dermatitis prevalence among the Chinese population (1990-2021) with projections for 2022-2030. *Pediatr Allergy Immunol*. 2024;35(10):e14271. doi:10.1111/pai.14271
4. Maurelli M, Chiricozzi A, Peris K, Gisondi P, Girolomoni G. Atopic dermatitis in the elderly population. *Acta Derm Venereol*. 2023;103:adv13363. doi:10.2340/actadv.v103.13363
5. Ferrara F, Zovi A, Capuozzo M, Langella R. Atopic dermatitis: treatment and innovations in immunotherapy. *Inflammopharmacology*. 2024;32(3):1777–1789. doi:10.1007/s10787-024-01453-8
6. Bosma AL, Ascott A, Iskandar R, et al. Classifying atopic dermatitis: a systematic review of phenotypes and associated characteristics. *J Eur Acad Dermatol Venereol*. 2022;36(6):807–819. doi:10.1111/jdv.18008
7. Chen B, Yang J, Song Y, Zhang D, Hao F. Skin immunosenescence and type 2 inflammation: a mini-review with an inflammaging perspective. *Front Cell Dev Biol*. 2022;10:835675. doi:10.3389/fcell.2022.835675
8. Siiskonen H, Harvima I. Mast cells and sensory nerves contribute to neurogenic inflammation and pruritus in chronic skin inflammation. *Front Cell Neurosci*. 2019;13:422. doi:10.3389/fncel.2019.00422
9. Roy S, Chompunud Na Ayudhya C, Thapaliya M, Deepak V, Ali H. Multifaceted MRGPRX2: new insight into the role of mast cells in health and disease. *J Allergy Clin Immunol*. 2021;148(2):293–308. doi:10.1016/j.jaci.2021.03.049
10. Kühn H, Kolkhir P, Babina M, et al. Mas-related G protein-coupled receptor X2 and its activators in dermatologic allergies. *J Allergy Clin Immunol*. 2021;147(2):456–469.
11. Zhang Y, Zhang M, Tang C, et al. Palmitoylation by ZDHHC4 inhibits TRPV1-mediated nociception. *EMBO Rep*. 2025;26(1):101–121.
12. Voisin T, Perner C, Messou MA, et al. The CysLT2R receptor mediates leukotriene C4-driven acute and chronic itch. *Proc Natl Acad Sci USA*. 2021;118(13):e2022087118. doi:10.1073/pnas.2022087118
13. Cevikbas F, Wang X, Akiyama T, et al. A sensory neuron-expressed IL-31 receptor mediates T helper cell-dependent itch: involvement of TRPV1 and TRPA1. *J Allergy Clin Immunol*. 2014;133(2):448–460. doi:10.1016/j.jaci.2013.10.048
14. Zhang L, Jiang GY, Song NJ, et al. Extracellular signal-regulated kinase (ERK) activation is required for itch sensation in the spinal cord. *Mol Brain*. 2014;7(1):25. doi:10.1186/1756-6606-7-25
15. Liu X, Wang Y, Tao T, et al. GRPR/extracellular signal-regulated kinase and NPRA/extracellular signal-regulated kinase signaling pathways play a critical role in spinal transmission of chronic itch. *J Invest Dermatol*. 2021;141(4):863–873. doi:10.1016/j.jid.2020.09.008
16. Innis SM. Palmitic acid in early human development. *Crit Rev Food Sci Nutr*. 2016;56(12):1952–1959. doi:10.1080/10408398.2015.1018045
17. Lin H. Protein cysteine palmitoylation in immunity and inflammation. *FEBS J*. 2021;288(24):7043–7059. doi:10.1111/febs.15728
18. Chen LY, Yang-Yen HF, Tsai CC, et al. Protein palmitoylation by ZDHHC13 protects skin against microbial-driven dermatitis. *J Invest Dermatol*. 2017;137(4):894–904. doi:10.1016/j.jid.2016.12.011
19. Chen LY, Lin KR, Chen YJ, et al. Palmitoyl acyltransferase activity of ZDHHC13 regulates skin barrier development partly by controlling padi3 and TGM1 protein stability. *J Invest Dermatol*. 2020;140(5):959–970.e3. doi:10.1016/j.jid.2019.09.017
20. Wang X, Liu JZ, Hu JX, et al. ROS-activated p38 MAPK/ERK-Akt cascade plays a central role in palmitic acid-stimulated hepatocyte proliferation. *Free Radic Biol Med*. 2011;51(2):539–551. doi:10.1016/j.freeradbiomed.2011.04.019
21. Me S, Bazinet RP. Unraveling brain palmitic acid: origin, levels and metabolic fate. *Prog Lipid Res*. 2024;96:101300.
22. Pantović R, Draganić P, Eraković V, Blagović B, Milin C, Simonić A. Effect of indomethacin on motor activity and spinal cord free fatty acid content after experimental spinal cord injury in rabbits. *Spinal Cord*. 2005;43(9):519–526. doi:10.1038/sj.sc.3101763
23. Moosbrugger-Martinz V, Schmuth M, Dubrac S. A mouse model for atopic dermatitis using topical application of vitamin D3 or of its analog MC903. *Methods Mol Biol*. 2017;1559:91–106.
24. Sengupta S, Azad RK. An RNA-Seq Data Analysis Pipeline. *Methods Mol Biol*. 2024;2812:1–9.
25. Liu B, Chen R, Wang J, et al. Exploring neuronal mechanisms involved in the scratching behavior of a mouse model of allergic contact dermatitis by transcriptomics. *Cell Mol Biol Lett*. 2022;27(1):16.
26. Ren Y, Yu G, Shi C, et al. Majorbio Cloud: a one-stop, comprehensive bioinformatic platform for multiomics analyses. *Imeta*. 2022;1(2):e12. doi:10.1002/imt2.12
27. Steinhoff M, Ahmad F, Pandey A, et al. Neuroimmune communication regulating pruritus in atopic dermatitis. *J Allergy Clin Immunol*. 2022;149(6):1875–1898. doi:10.1016/j.jaci.2022.03.010
28. Marek-Jozefowicz L, Nedoszytko B, Grochocka M, et al. Molecular mechanisms of neurogenic inflammation of the skin. *Int J Mol Sci*. 2023;24(5):5001. doi:10.3390/ijms24055001
29. Arai I, Saito S. Interleukin-31 receptor a expression in the dorsal root ganglion of mice with atopic dermatitis. *Int J Mol Sci*. 2023;24(2):1047. doi:10.3390/ijms24021047
30. Misery L, Pierre O, Le Gall-Ianotto C, et al. Basic mechanisms of itch. *J Allergy Clin Immunol*. 2023;152(1):11–23. doi:10.1016/j.jaci.2023.05.004
31. Lay M, Dong X. Neural mechanisms of itch. *Annu Rev Neurosci*. 2020;43(1):187–205. doi:10.1146/annurev-neuro-083019-024537
32. Barry DM, Munanairi A, Chen ZF. Spinal mechanisms of itch transmission. *Neurosci Bull*. 2018;34(1):156–164. doi:10.1007/s12264-017-0125-2
33. Chen XJ, Sun YG. Central circuit mechanisms of itch. *Nat Commun*. 2020;11(1):3052. doi:10.1038/s41467-020-16859-5
34. Chen PY, Shen M, Cai SQ, Tang ZW. Association between atopic dermatitis and aging: clinical observations and underlying mechanisms. *J Inflamm Res*. 2024;17:3433–3448. doi:10.2147/JIR.S467099
35. Li F, Xie W, Chen Z, et al. Neuropeptide Y and receptors are associated with the pyroptosis of nucleus pulposus in aging and degenerative intervertebral discs of rats. *Neuropeptides*. 2022;96:102284. doi:10.1016/j.npep.2022.102284
36. Teng Y, Zhong H, Yang X, Tao X, Fan Y. Current and emerging therapies for atopic dermatitis in the elderly. *Clin Interv Aging*. 2023;18:1641–1652. doi:10.2147/CIA.S426044
37. Ewan EE, Avraham O, Carlin D, Gonçalves TM, Zhao G, Cavalli V. Ascending dorsal column sensory neurons respond to spinal cord injury and downregulate genes related to lipid metabolism. *Sci Rep*. 2021;11(1):374. doi:10.1038/s41598-020-79624-0
38. Paterniti I, Impellizzeri D, Crupi R, et al. Molecular evidence for the involvement of PPAR-δ and PPAR-γ in anti-inflammatory and neuroprotective activities of palmitoylethanolamide after spinal cord trauma. *J Neuroinflammation*. 2013;10(1):20. doi:10.1186/1742-2094-10-20

39. Moon PD, Han NR, Kim HM, Jeong HJ. High-fat diet exacerbates dermatitis through up-regulation of TSLP. *J Invest Dermatol*. 2019;139 (5):1198–1201. doi:10.1016/j.jid.2018.11.003
40. Yu J, Song P, Bai Y, et al. CD36-SREBP1 axis mediates tslp production in obesity-exacerbated atopic dermatitis. *J Invest Dermatol*. 2023;143 (11):2153–2162.e12. doi:10.1016/j.jid.2023.04.024
41. Dimasuay KG, Berg B, Schaunaman N, Holguin F, Winnica D, Chu HW. High-fat diet and palmitic acid amplify airway type 2 inflammation. *Front Allergy*. 2023;4:1193480. doi:10.3389/falgy.2023.1193480
42. Korbecki J, Bajdak-Rusinek K. The effect of palmitic acid on inflammatory response in macrophages: an overview of molecular mechanisms. *Inflamm Res*. 2019;68(11):915–932. doi:10.1007/s00011-019-01273-5
43. Zylka MJ, Rice FL, Anderson DJ. Topographically distinct epidermal nociceptive circuits revealed by axonal tracers targeted to Mrgprd. *Neuron*. 2005;45(1):17–25. doi:10.1016/j.neuron.2004.12.015
44. Guo C, Jiang H, Huang CC, et al. Pain and itch coding mechanisms of polymodal sensory neurons. *Cell Rep*. 2023;42(11):113316. doi:10.1016/j.celrep.2023.113316
45. Wang C, Liu Y, Lanier M, et al. High-affinity agonists reveal recognition motifs for the MRGPRD GPCR. *Cell Rep*. 2024;43(12):114942. doi:10.1016/j.celrep.2024.114942
46. Qu L, Fan N, Ma C, et al. Enhanced excitability of MRGPRA3- and MRGPRD-positive nociceptors in a model of inflammatory itch and pain. *Brain*. 2014;137(Pt 4):1039–1050. doi:10.1093/brain/awu007
47. Klein A, Solinski HJ, Malewicz NM, et al. Pruriception and neuronal coding in nociceptor subtypes in human and nonhuman primates. *Elife*. 2021;10:e64506. doi:10.7554/eLife.64506
48. Zhang S, Lin H, Wang J, et al. Sensing ceramides by CYSLTR2 and P2RY6 to aggravate atherosclerosis. *Nature*. 2025;641(8062)):476–485. doi:10.1038/s41586-025-08792-8
49. Wang F, Trier AM, Li F, et al. A basophil-neuronal axis promotes itch. *Cell*. 2021;184(2):422–440.e17. doi:10.1016/j.cell.2020.12.033
50. Matsuo S, Hashimoto T, Matsuura F, et al. Central, but not peripheral, nervous system ERK2 is essential for itch signals in murine allergic skin inflammation. *Allergy*. 2021;76(11):3422–3432. doi:10.1111/all.14867
51. Liu W, Luo Y, Song W, et al. Angelica Yinzi alleviates pruritus-related atopic dermatitis through skin repair, antioxidation, and balancing peripheral μ - and κ -opioid Receptors. *Evid Based Complement Alternat Med*. 2023;2023(1):6058951. doi:10.1155/2023/6058951
52. Sun PY, Li HG, Xu QY, et al. Lidocaine alleviates inflammation and pruritus in atopic dermatitis by blocking different population of sensory neurons. *Br J Pharmacol*. 2023;180(10):1339–1361. doi:10.1111/bph.16012
53. Zhang L, Tanabe K, Yanagidate F, et al. Different effects of local anesthetics on extracellular signal-regulated kinase phosphorylation in rat dorsal horn neurons. *Eur J Pharmacol*. 2014;734:132–136. doi:10.1016/j.ejphar.2014.03.048
54. Deane C. Lipids: picturing palmitoylation. *Nat Chem Biol*. 2018;14(3):199. doi:10.1038/nchembio.2577
55. Wang C, Chen X, Shi W, et al. 2-Bromopalmitate impairs neural stem/progenitor cell proliferation, promotes cell apoptosis and induces malformation in zebrafish embryonic brain. *Neurotoxicol Teratol*. 2015;50:53–63. doi:10.1016/j.ntt.2015.06.001
56. Wang C, Cui ZY, Chang HY, et al. 2-Bromopalmitate inhibits malignant behaviors of HPSCC cells by hindering the membrane location of Ras protein. *Exp Biol Med*. 2023;248(23):2393–2407. doi:10.1177/15353702231220671